Sub-10 μm grain size, $Ba_{1-x}Ca_xTi_{0.9}Zr_{0.1}O_3$ (x = 0.10 and x = 0.15) piezoceramics processed using a reduced thermal treatment

2015 Smart Mater. Struct. 24 065033

(http://iopscience.iop.org/0964-1726/24/6/065033)

IOP Publishing Smart Materials and Structures
Smart Mater. Struct. **24** (2015) 065033 (8pp) doi:10.1088/0964-1726/24/6/065033

Sub-10 μm grain size, $Ba_{1-x}Ca_xTi_{0.9}Zr_{0.1}O_3$ ($x = 0.10$ and $x = 0.15$) piezoceramics processed using a reduced thermal treatment

A Reyes-Montero[1], L Pardo[2], R López-Juárez[3], A M González[4], S O Rea-López[1], M P Cruz[5] and M E Villafuerte-Castrejón[1]

[1] Instituto de Investigaciones en Materiales, Universidad Nacional Autónoma de México, Circuito Exterior S/N, A.P. 70-360, México, D.F., Mexico
[2] Instituto de Ciencia de Materiales de Madrid, ICMM-CSIC, Sor Juana Inés de la Cruz, 3. Cantoblanco, 28049 Madrid, Spain
[3] Unidad Morelia del Instituto de Investigaciones en Materiales, Universidad Nacional Autónoma de México, Antigua Carretera a Pátzcuaro No. 8701, Col. Ex Hacienda de San José de la Huerta, C.P. 58190, Morelia, Michoacán, Mexico
[4] Grupo POEMMA, ETSIS Telecomunicación, Campus Sur, Universidad Politécnica de Madrid, Ctra. Valencia Km 7, 28031 Madrid, Spain
[5] Centro de Nanociencias y Nanotecnología, Universidad Nacional Autónoma de México, Km. 107, Carretera Tijuana-Ensenada, C.P. 22800, Ensenada, B. C., Mexico

E-mail: ingaremo@gmail.com

Received 30 March 2015, revised 18 April 2015
Accepted for publication 20 April 2015
Published 18 May 2015

Abstract

The solid-state synthesis of $Ba_{1-x}Ca_xTi_{0.9}Zr_{0.1}O_3$ ($x = 0.10$, 0.15) (BCTZ) powder and the processing method of ceramics, by the use of reduced synthesis time and temperature (1250 °C for 2 h), are reported. Homogeneous and dense (⩾95%) ceramic microstructures with sub-10 μm grain size were obtained under all sintering conditions. A comparative study of their ferro-piezoelectric properties as a function of sintering temperatures is presented. The study shows the role of the grain size effect for improving both piezoelectric and ferroelectric properties of these materials. With an increase of the sintering temperature, grain growth was promoted; therefore, higher ferro-piezoelectric values were obtained (at 1400 °C, for $x = 0.10$: $d_{33} = 300$ pC/N, $d_{31} = -150$ pC/N, $k_p = 48\%$; for $x = 0.15$: $d_{33} = 410$ pC/N, $d_{31} = -154$ pC/N, $k_p = 50\%$). In addition, a diffuse phase transition is observed in these BCTZ ceramics with a Curie temperature near 100 °C at 1 kHz.

Keywords: BCTZ solid solutions, ferroelectrics, piezoelectrics

(Some figures may appear in colour only in the online journal)

1. Introduction

Nowadays, and due to the increasing importance of environmental protection, research on piezoelectric and ferroelectric materials has been focused on lead-free ceramics development, for which some objectives of industrial transference have already been achieved, whereas some basic problems remain still unsolved [1]. Barium titanate (BT) binary systems [2–5] have been widely studied due to their non-toxicity and aim to overcome the main issues for practical applications, i.e., its low Curie temperature ($T_C \approx 120$ °C) and electromechanical coupling factor ($k_p \approx 35\%$).

BT undergoes three known structural phase transformations. Substituting the A and/or B sites of the BT perovskite structure makes it possible to modify its phase transition

temperature. The addition of Ca^{2+} into the Ba^{2+} site increases the stability temperature range of the tetragonal phase [2] by displacing the rhombohedral (R) to the orthorhombic (O) (T_1) and the orthorhombic (O) to the tetragonal (T) (T_2) ferroelectric-ferroelectric (FE) phases' transition temperatures. An optimum amount of Ca^{+2} ($0.06 < x < 0.10$) enhances the dielectric properties of BCTZ materials [6]. The substitution of Zr^{4+} into Ti^{4+} sites in $Ba(Ti_{1-y}Zr_y)O_3$ produces the shift toward a lower temperature of the tetragonal to cubic phase transition, i.e., ferroelectric to paraelectric transition at T_C, while the other two FE to FE phases' transition temperatures (T_1 and T_2) increase at different rates. For $y = 0.15$, three ferroelectric phases (R, O and T) coexist near room temperature. It was expected to see a great polarizability at the pinched point; however, no ferroelectric and piezoelectric improvement was achieved. This was probably due to the degradation of ferroelectricity and weak ferroelectric-relaxor behavior at this level of Zr^{4+} content [3]. Furthermore, the ceramic shows broad dielectric peaks with frequency dispersion, i.e., ferroelectric relaxor behavior with increasing the Zr^{4+} concentration ($y > 0.25$) [4, 5]. Recent work suggested a phase coexistence between $0.02 > y > 0.05$ and $0.07 < y < 0.09$ due to two polymorphic phase transitions, resulting in enhanced piezoelectric properties (225 pC/N $< d_{33} <$ 295 pC/N) [7].

Lately, pseudo-binary systems with high piezoelectric sensitivity (Ba,Ca)(Zr,Ti)O_3 have been successfully developed as promising candidates for lead-free piezoelectric ceramics [8–10]. Among the drawbacks that exist in compositions with the highest piezoelectric activity ($x = 0.15$ $y = 0.10$; $d_{33} \approx 620$ pC/N) are the low $T_C \approx 93$ °C, high synthesis (1300 °C for 2 h) and sintering (1450 °C for 3 h) conditions (not suitable for industrial production) and the subsequently large grain structures. Microstructures with average grain size >10 μm obtained to date are not optimized for the present trend of device miniaturization. This feature result is important in order to increase the frequency range of the ultrasonic transduction. Therefore, strategies to reduce the synthesis and sintering temperatures are needed for processing routes towards sub-10 μm grain size ceramics.

Some efforts have been dedicated to reducing the materials' processing temperature [11] using conventional ceramic methods and employing different modifying agents, i.e., $Ba_{0.85}Ca_{0.15}Ti_{0.90}Zr_{0.10}O_3$ ceramics with CeO_2 added, calcined at 1250 °C for 2 h and sintered at 1350 °C for 4 h, showed a piezoelectric coefficient $d_{33} \approx 600$ pC/N [12]. Moreover, $Ba_{0.85}Ca_{0.15}Ti_{0.90}Zr_{0.10}O_3$ ceramics with MnO added, calcined at 1100 °C for 4 h and sintered at 1350 °C for 2 h, exhibited a piezoelectric coefficient $d_{33} \approx 373$ pC/N [13]. Besides, LiF doping was used to reduce the sintering temperature at the expense of lower piezoelectric properties [14]. The authors recently achieved good piezoelectric properties in ceramics processed below 1300 °C using the Pechini method [15].

In this work, we explore the possibility of optimizing the ceramic microstructure by a conventional solid-state technique using moderate sintering conditions, while keeping piezoelectric properties high enough for practical uses. Investigations were carried out for $Ba_{1-x}Ca_xTi_{0.9}Zr_{0.1}O_3$ ceramics with $x = 0.10$ and 0.15, since their good piezoelectric properties were recently reported using conventional processing routes [8, 9, 16, 17]. The relationship between structure and electrical properties is discussed. The effects of the sintering conditions over structure and ferro-piezoelectric properties are also reported.

2. Experimental details

$Ba_{1-x}Ca_xTi_{0.9}Zr_{0.1}O_3$ ($x = 0.10$ and 0.15) ceramics were prepared by solid-state synthesis. The starting materials were $BaCO_3$ (99.0%, Analytica), $CaCO_3$ (99.0%, Fluka), TiO_2 (99.0%, Aldrich) and ZrO_2 (99.0%, Riedel-deHaën). Stoichiometric amounts of reagents were weighted and mixed with acetone for 30 min. They were calcined at 1250 °C for 2 h. Afterwards, powders were ball milled for 24 h with zirconia ball media and alcohol, pressed into ~13.0 mm diameter and ~1.5 mm thickness pellets and sintered at 1300 °C, 1350 °C and 1400 °C for 2 h.

The phase structure of BCTZ ceramics was analyzed using x-ray diffraction with a Cu kα1 radiation (1.54178 Å, Bruker D8 Advance with a 0.016° step size in 2θ and 1 s of integration time). Morphology of the samples was studied by a field emission scanning electron microscope (SEM) (JEOL J7600f) and computer-aided image analysis with Image J software. The average grain size of a large sample area was determined by the interception method.

Samples used for piezoelectric and dielectric characterization were polished and silver paste was applied on both sides of the samples at 700 °C for 10 min to form electrodes.

Dielectric permittivity (ε_{33}^{T}) and losses (tan δ) were measured with a precision impedance analyzer (Agilent 4294A) from room temperature up to 180 °C. Then, ceramics were poled at 2 kV mm^{-1} for 30 min at room temperature. Piezoelectric constants d_{33} and $-d_{31}$ were measured using a wide-range d_{33}-meter (APC International). Electromechanical coupling factor k_p, elastic compliances s_{11}^{E}, s_{12}^{E} and piezoelectric constants $-g_{31}$, g_{33} were calculated using the resonance method and an automatic iterative analysis method of complex impedance at the radial mode of the disks [18]. The piezoelectric properties were measured after 24 h of the poling process. Ferroelectric hysteresis loops were measured at room temperature using a Radiant workstation at 100 Hz.

3. Results and discussion

Figure 1 shows the x-ray diffraction (XRD) patterns of $Ba_{1-x}Ca_xTi_{0.9}Zr_{0.1}O_3$ ($x = 0.10$ and 0.15) calcined powders at 1250 °C for 2 h and those of sintered ceramics at different temperatures. The powders have traces of secondary phases, which indicates the fact that all reactions were not completed at this temperature and they are still reactive upon further thermal treatments, thus enhancing sintering. The samples showed a single perovskite phase crystal structure, and the diffraction peaks of the samples were

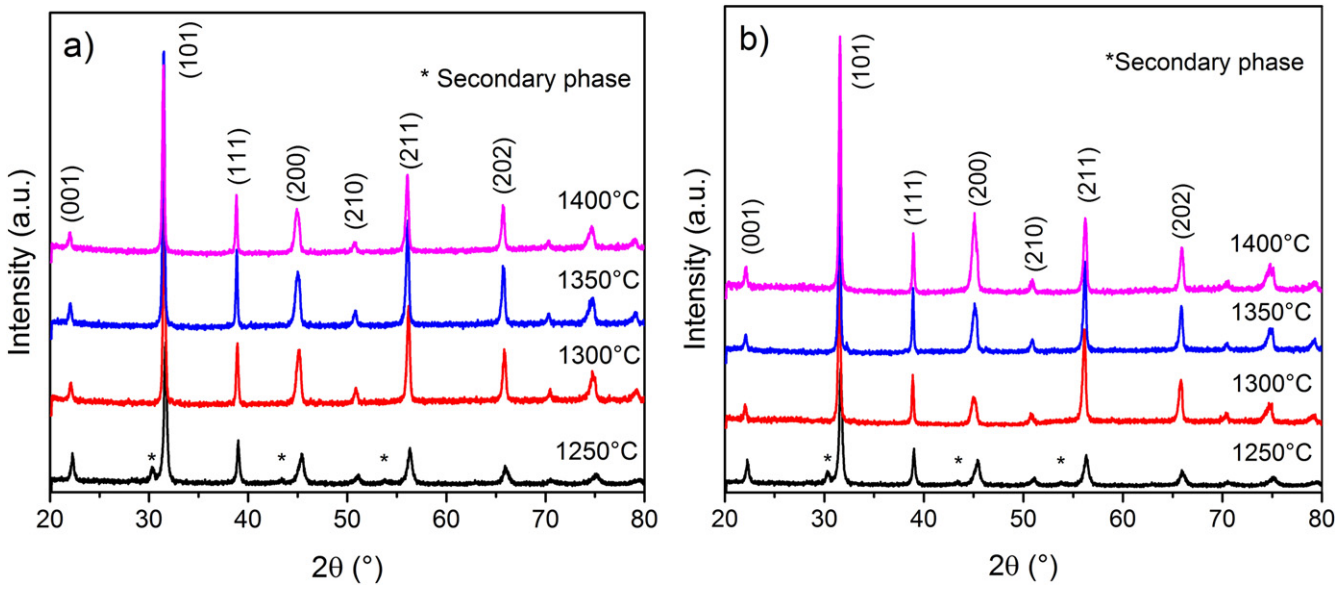

Figure 1. XRD patterns of BCTZ ceramics synthesized at 1250 °C and sintered at 1300, 1350, 1400 °C: (a) $x = 0.10$ and (b) $x = 0.15$.

indexed to the perovskite-type cubic prototype structure. XRD patterns indicate that Ca^{2+} and Zr^{4+} ions incorporate to the $BaTiO_3$ lattice to form a solid solution.

The crystal structure of pure $BaTi_{0.9}Zr_{0.10}O_3$ at room temperature is rhombohedral [3], which is indicated by the single (200) peak, the doublet (111)/(–111) and the small (311) peak. With the increase of Ca^{2+} content, pronounced splitting of the (002) peak from the (200) peak has been observed, demonstrating a phase transition from the rhombohedral to tetragonal phase [16], which is stabilized at room temperature by the substitution of Ba^{2+} by Ca^{2+}. Then, it was speculated that the rhombohedral and tetragonal phases may coexist in the composition range $x = 0.10$–0.20 and consequently, the existence of a temperature-independent morphotropic phase boundary (MPB). However, more structural data as a function of the temperature is still needed to assure this point and disregard other options [19]. An example of such an option is the existence of a polymorphic phase transition (PPT) and a tricritical point close to room temperature, i.e., a temperature for the coexistence of the cubic paraelectric high-temperature phase and two ferroelectric phases.

In our samples, for both Ca^{2+} compositions, the possible coexisting rhombohedral and tetragonal phases would have feeble distortions from the cubic prototype perovskite structure, featured with the merging of the (111)/(–111) and (002)/(200) doublets into single peaks around 38° and 45° in 2θ, respectively (figure 2). Such a pseudo-cubic structure is not compatible with the ferro-piezoelectric performance. This global structure observed in the ceramics here studied could, on the other hand, average a range of local polar configurations [20]. Both global and short-range structures are needed to understand the structural response. However, this is beyond the scope of this work.

Figure 3 shows the SEM micrographs of $x = 0.10$ and $x = 0.15$ BCTZ ceramics sintered at different temperatures. As shown, the grain size increases with the sintering temperature [10, 21] due to a higher mass transport, resulting in high densification (>90% calculated from the XRD data). Moreover, it is reported that the Zr^{4+} content helps to improve the grain growth of the BCTZ ceramics [16]. The increase in crystal size makes it easier to switch the domains, as will be discussed later. In this work the average grain size is around 0.5, 3.2, 11.1 μm for $x = 0.10$ and 0.5, 2.1, 8.7 μm for $x = 0.15$ at 1300, 1350 and 1400 °C, respectively.

Figure 4 shows the dependence of dielectric permittivity and losses as a function of temperature for BCTZ ceramics sintered at 1400 °C. Wide permittivity peaks indicate that a diffuse phase transition is presented. In addition to the permittivity maxima related with the transition to the paraelectric phase, there is another wide transition at lower temperatures, around 40 °C. This indicates that the transition between rhombohedral and orthorhombic and between orthorhombic to tetragonal ferroelectric phases merge into a unique one [17], suggesting a coexistence of symmetries near this temperature. This effect leads to a higher number of grains being oriented favorable towards the electric field, a well-known phenomenon at the MPB.

Figure 5 displays the dielectric permittivity and losses between the two compositions under investigation. The effect that Ca^{2+} doping has over the phase transition and the Curie temperature of the ceramics is compared. In the present study, the results for dielectric permittivity correspond to previous reports [10, 22] for approximately the same grain size.

A diffuse phase transition is generally characterized by (a) broadening in the dielectric permittivity versus temperature curve; (b) a relative large separation (in temperature) between the maximum of the real dielectric constant and imaginary dielectric loss parts; (c) a deviation from the Curie–Weiss law near the maximum dielectric permittivity (T_m); and (d) frequency dispersion of both ε and tan δ in the transition region [23].

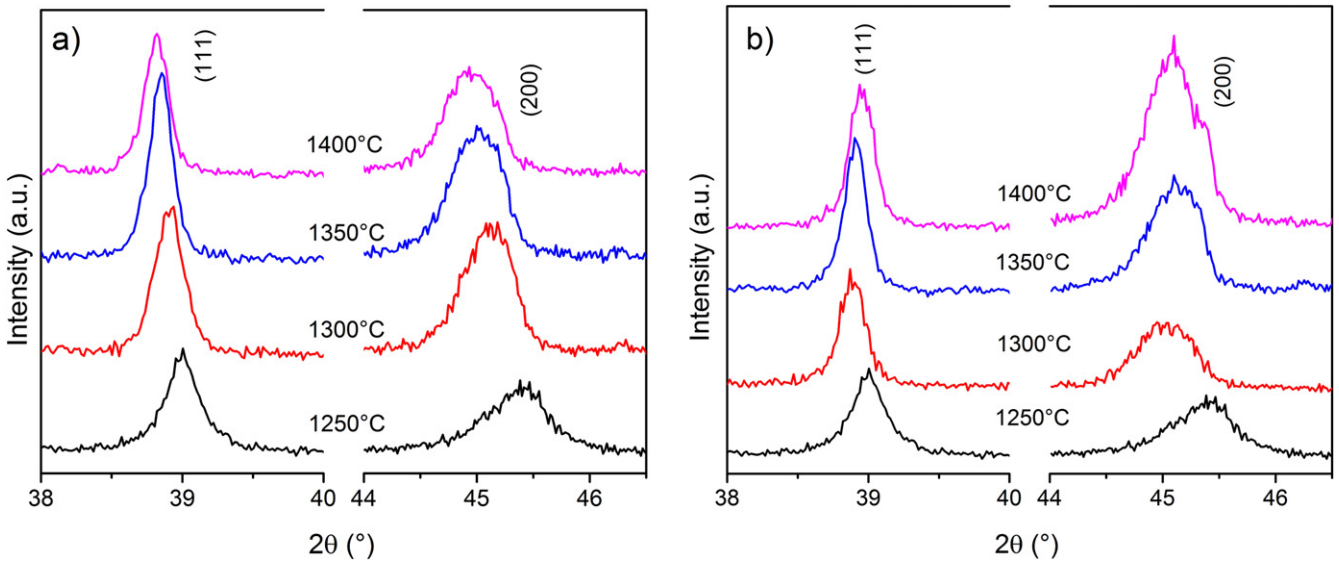

Figure 2. Magnification of the (111) and (200) peaks at the XRD patterns of BCTZ ceramics synthesized at 1250 °C and sintered at 1300, 1350, 1400 °C: (a) $x = 0.10$ and (b) $x = 0.15$.

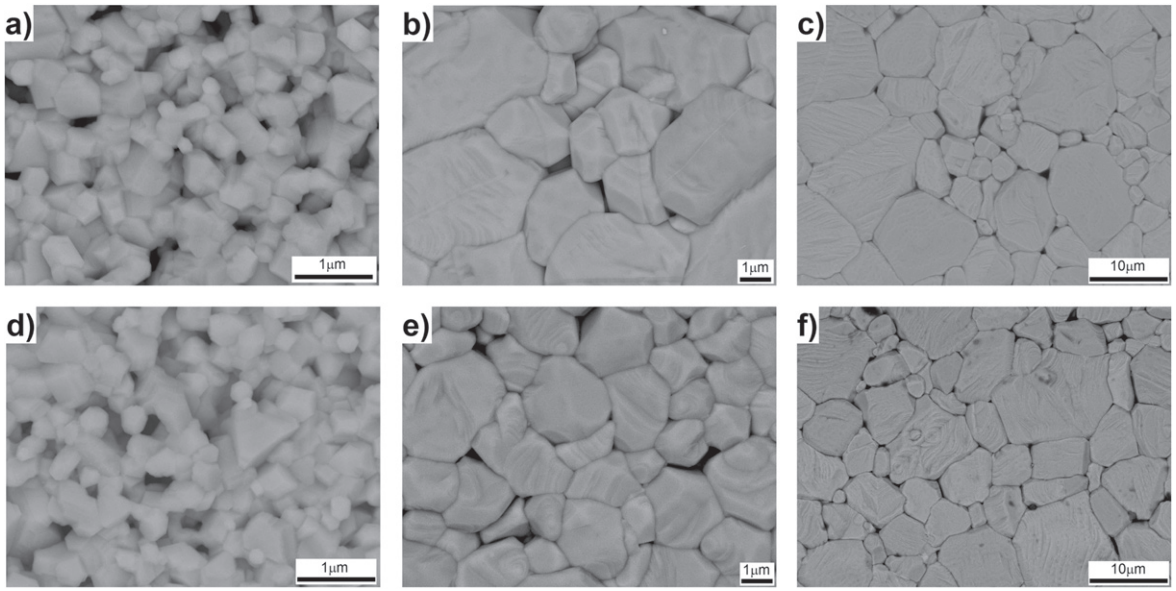

Figure 3. SEM micrographs of BCTZ sintered ceramics: $x = 0.10$ (a) 1300 °C (b) 1350 °C (c) 1400 °C; $x = 0.15$ (d) 1300 °C (e) 1350 °C (f) 1400 °C.

The dielectric permittivity of a normal ferroelectric above Curie temperature follows the Curie–Weiss law described by:

$$\frac{1}{\varepsilon} = \frac{T - T_0}{C} \quad (T > T_c) \tag{1}$$

where T_0 is the Curie–Weiss temperature and C is the Curie–Weiss constant. Figure 6 shows the plots of inverse dielectric permittivity of BCTZ ceramics (1400 °C) at 1 kHz versus temperature. Their respective insets correspond to the curves of log ($1/\varepsilon$—$1/\varepsilon_m$) against log (T—T_m) at 1 kHz.

Usually, for a well-known 'normal' ferroelectric, the temperature of the maximum T_m corresponds to the ferroelectric-paraelectric phase transition temperature. Furthermore, the parameter ΔT_m describes the degree of the deviation from the Curie–Weiss law:

$$\Delta T_m = T_{cw} - T_m \tag{2}$$

where T_{cw} denotes the temperature from which the dielectric permittivity starts to deviate from the Curie–Weiss law and T_m represents the temperature of the dielectric maximum.

A modified Curie–Weiss expression [24] is proposed to describe the diffuseness of a phase transition:

$$\frac{1}{\varepsilon} - \frac{1}{\varepsilon_m} = \frac{(T - T_m)^\gamma}{C} \tag{3}$$

where γ (diffusion coefficient ranging) and C are assumed to be constant. The parameter γ gives information on the character of the phase transition: $\gamma = 1$ a normal Curie–Weis

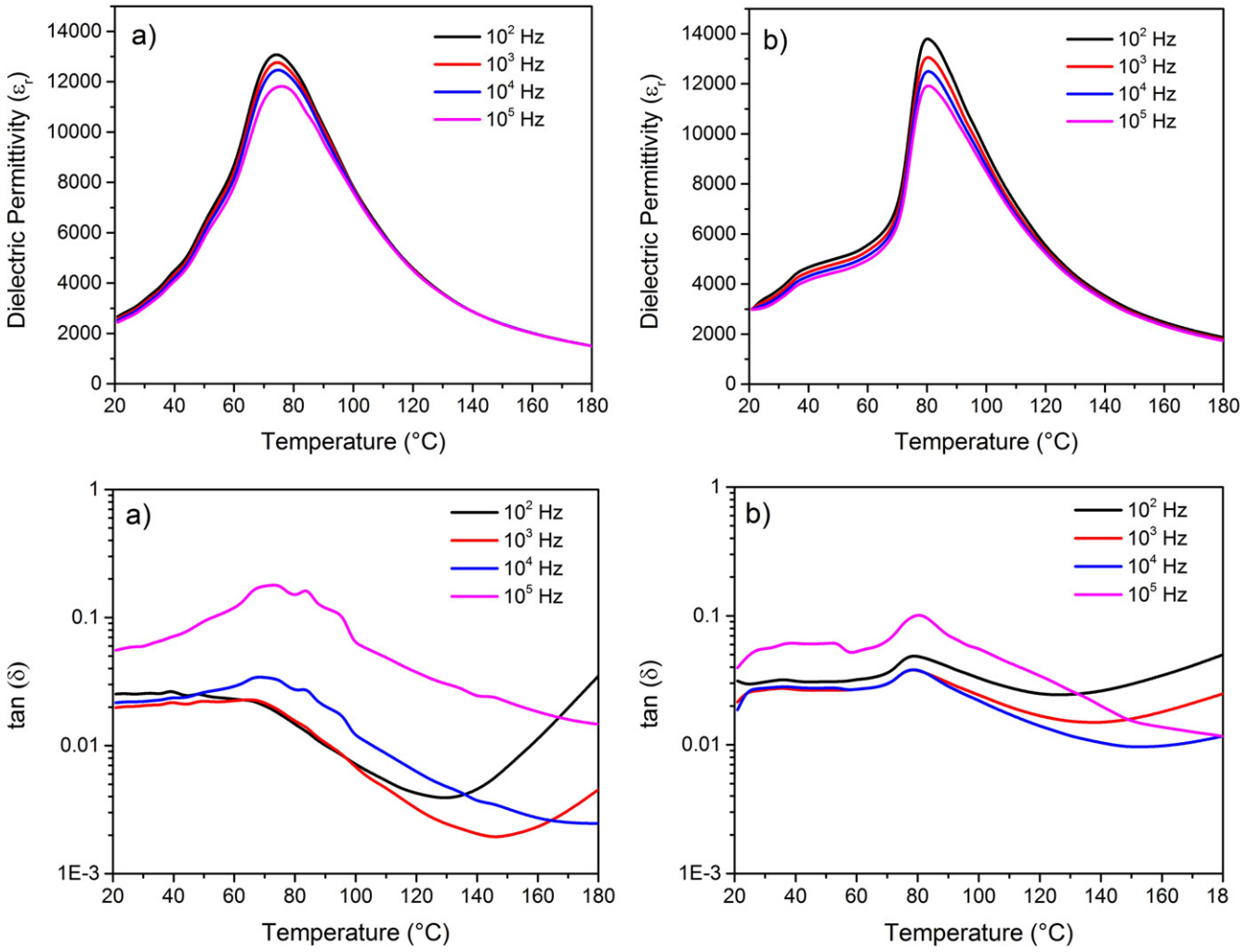

Figure 4. Dielectric permittivity and losses for BCTZ sintered ceramics (1400 °C): (a) $x = 0.10$; (b) $x = 0.15$.

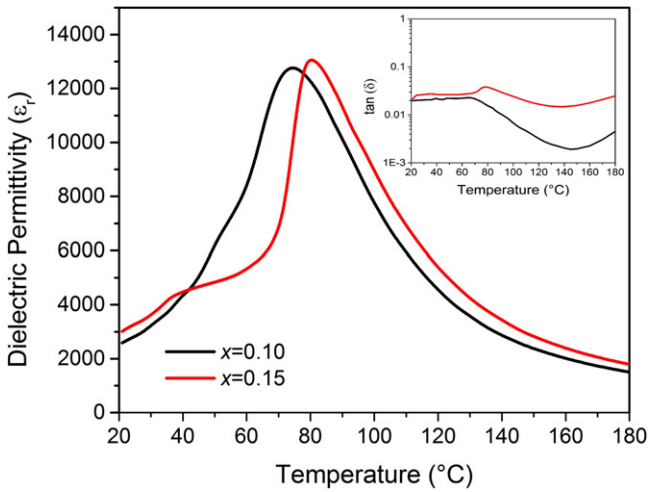

Figure 5. Comparative plots for dielectric permittivity and losses (inset) in BCTZ ceramics (1400 °C) at 1 kHz.

law (normal ferroelectric); $\gamma = 2$ describes a complete diffuse phase transition (ideal relaxor ferroelectric). A linear relationship for both BCTZ compositions was obtained (figure 6). The γ values indicate that transitions are a diffuse-like type. Table 1 shows the C and γ values calculated for BCTZ ceramics in addition with a summary of the fitting parameters obtained from equations (1)–(3).

Values for T_0, T_{cw}, and T_m, for these BCTZ ceramics are in the same trend. Moreover, the C constant follows the same tendency for various grain sizes reported with BCTZ [10]. However, the γ coefficient for these BCTZ studies indicates that ceramics with $x = 0.10$ compositions show a higher relaxor character.

Hysteresis loops for BCTZ ceramics are shown in figure 7. Remnant polarization (P_r) of BCTZ ceramics at $x = 0.10$ is slightly higher than for $x = 0.15$. Furthermore, it increases with the sintering temperature. This phenomenon can be related to the easy switching of the ferroelectric domains by increasing the grain size. Table 2 shows the remnant polarization and coercive field for BCTZ ceramics sintered at different temperatures. The coercive field indicates that the ceramic is 'soft' in relation to the electric field because the free energy profile of the polarization rotation is anisotropically flattened at this phase boundary [8]. Furthermore, the existence of 90° domain walls diminishes the strain in sintered ceramics [10]. This effect also modifies the piezoelectric properties, increasing with a bigger domain size.

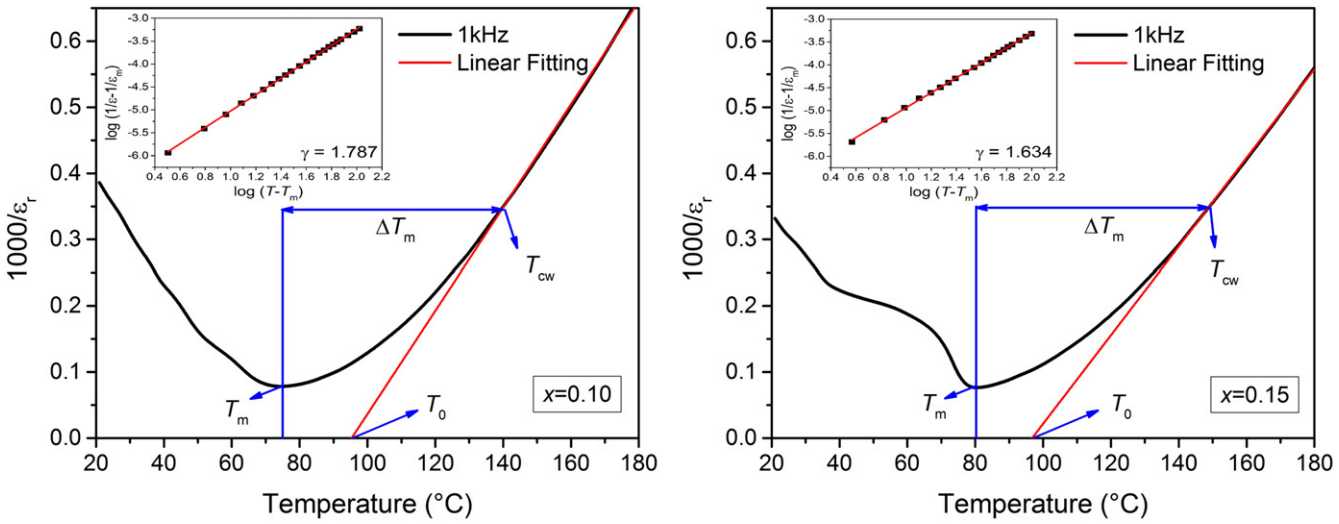

Figure 6. Inverse dielectric permittivity ($1000/\varepsilon_r$) as a function of temperature at 1 kHz, for BCTZ ceramics sintered at 1400 °C. Insets show the plot of $\log(1/\varepsilon—1/\varepsilon_m)$ versus $\log(T—T_m)$ (symbols: experimental data, solid line: fitting to equation (3)).

Table 1. Summary of fitting parameters for dielectric behavior and anomalies in obtained BCTZ ceramics.

BCTZ	T_0 (ºC)	T_{cw} (ºC)	T_m (ºC)	ΔT_m (ºC)	$C\times10^5$ (ºC)	γ
$x=0.10$	95.3	140.2	74.8	65.4	1.539	1.787
$x=0.15$	97.2	148.9	80.3	68.6	1.799	1.634

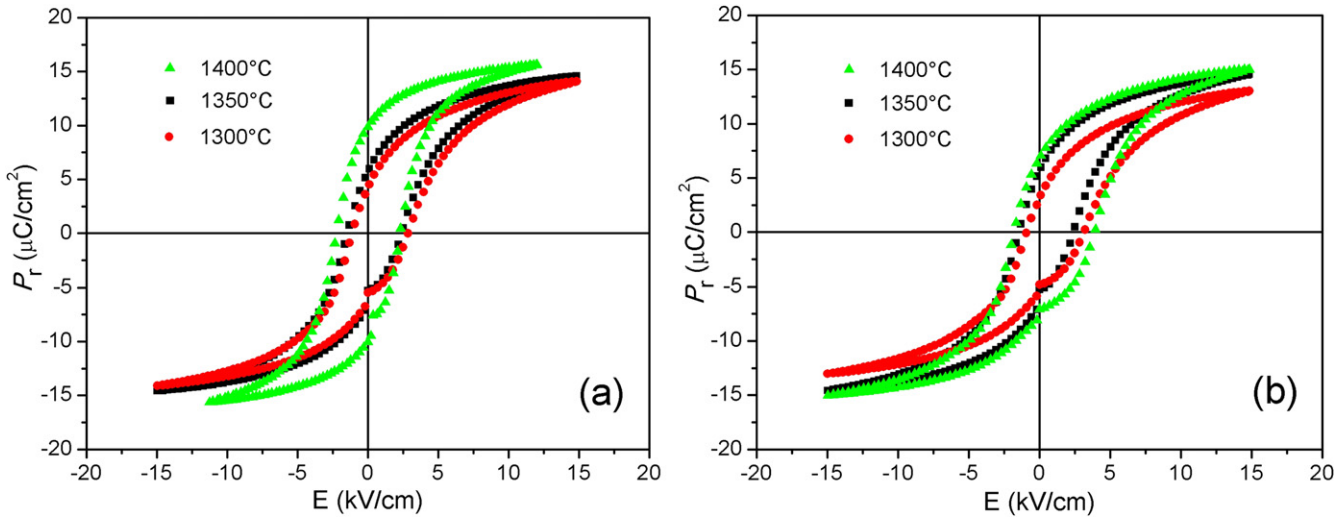

Figure 7. Ferroelectric loops of BCTZ ceramics at different sintering temperatures: (a) $x=0.10$ and (b) $x=0.15$.

Table 2. Pr and EC values from obtained BCTZ ceramics.

Sample (x)	Sintering temperature °C	P_r μC cm^{-2}	E_c kV cm^{-1}
0.10	1300	4.22	2.33
	1350	5.72	2.39
	1400	9.86	2.84
0.15	1300	3.39	3.96
	1350	5.44	2.40
	1400	7.05	3.22

Table 3 summarizes the piezoelectric properties obtained for BCTZ ceramics. As seen, there exist some differences with those reported in the literature due to diverse factors [10]: intrinsic microstructural properties such as grain size, density and chemical homogeneities; measurement parameters such as frequency, maximum electric field, and temperature; and the measurement method.

Figure 8 shows the radial resonance spectra for both compositions sintered at 1400 °C for 2 h. The phase angle (θ) value is correlated to the d_{33}. In this work a more square-like resonance is demonstrated for the $x=0.15$ ceramic; then the higher the θ value, the larger the d_{33} activity.

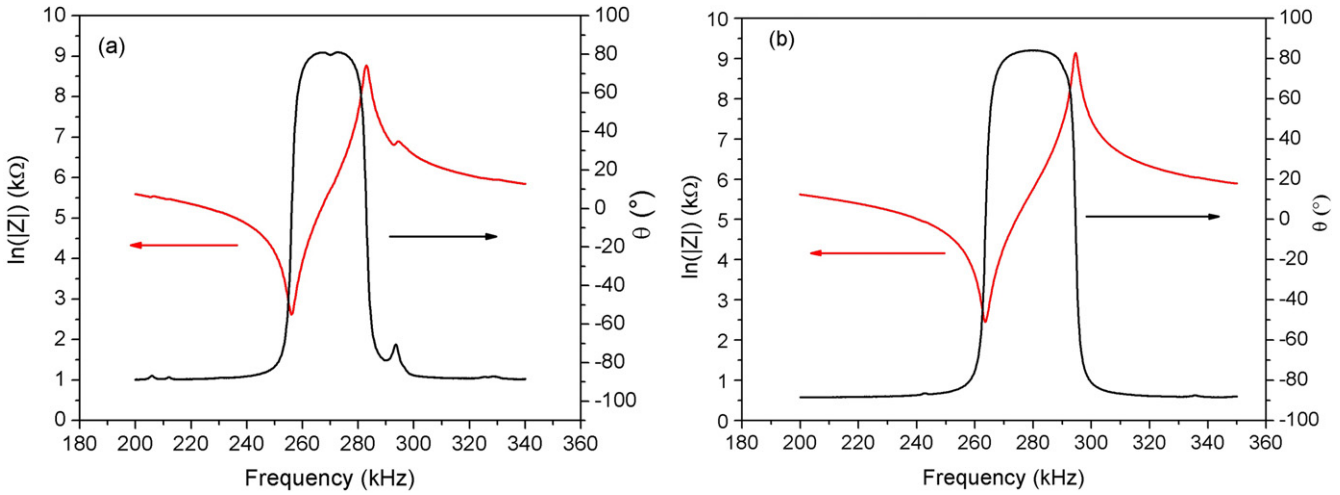

Figure 8. Radial resonance spectra for BCTZ ceramics sintered at 1400 °C: (a) $x = 0.10$ and (b) $x = 0.15$.

Table 3. Summary of piezoelectric properties from obtained BCTZ ceramics.

Sample	Sintering temperature	ρ	d_{33}	$-d_{31}$	k_p	s_{11}^E	$-s_{12}^E$	g_{33}	$-g_{31}$
(x)	°C	%	10^{-12} C N^{-1}	10^{-12} C N^{-1}	%	10^{-12} m^2 N^{-1}	10^{-12} m^2 N^{-1}	10^{-3} Vm N^{-1}	10^{-3} Vm N^{-1}
	1300	94	175	69	22	11.8	4.3	6.6	2.6
0.10	1350	95	285	96	31	11.3	3.4	11.7	4.0
	1400	97	300	150	48	11.0	3.3	11.9	5.3
	1300	96	210	78	27	14.1	7.4	8.4	3.1
0.15	1350	97	330	132	44	11.7	4.3	13.5	5.4
	1400	98	410	154	50	10.8	3.1	16.3	6.1

Although there are small differences in density among the samples sintered at different temperatures for both compositions, the piezoelectric performance drastically changes. Making a comparison between samples sintered at 1400 °C, the d_{33} value for $x = 0.15$ is higher than the value obtained for $x = 0.10$, despite both showing a square-like shape of radial resonance. Moreover, as temperature increases for $x = 0.15$ the d_{33} value is almost doubled. The same trend is observed for d_{31} and k_p. As mentioned earlier, it seems that the grain size has more influence over the piezoelectric properties than the density, since all the obtained ceramics are dense enough (theoretical density for $x = 0.10$: 5.83 g cm^{-3} and $x = 0.15$: 5.75 g cm^{-3}). This effect could be assigned to the contribution of 90° ferroelectric domains in ceramics with large crystals [10], as it enables the switching/rotation of the polarization vector.

4. Conclusions

BCTZ ceramics were obtained by solid-state synthesis using a reduced thermal treatment at 1250 °C (2 h) and different sintering temperatures (1300, 1350, 1400 °C for 2 h). Two compositions were studied ($x = 0.10$, $x = 0.15$). Both systems show a single perovskite phase type structure observed by x-ray diffraction analysis. It was found that in both compositions, ceramics sintered at 1400 °C exhibit excellent piezoelectric and ferroelectric properties due to an average increase in grain size, which promotes the ceramic polarization. From our results, it is also worth noting the production of high-sensitivity ($d_{33} > 250$ pC/N) piezoelectric ceramic bodies of the two compositions using a conventional solid-state synthesis method and temperature times as low as 1350 °C for 2 h with dense microstructure and average grain size in the 1 μm range. These BCTZ ceramics are promising candidates for many electronic micro-devices.

Acknowledgments

Armando Reyes wants to thank CONACyT-México for providing a scholarship, also Omar Novelo (IIM-UNAM) for SEM image acquisition and Adriana Tejeda (IIM-UNAM) for x-ray pattern data. M E Villafuerte-Castrejón kindly acknowledges CONACyT CB-2011-1 No.166108 and PAPIIT-UNAM (IN102715) for financial support. L Pardo acknowledges support of CSIC-PIE 201060E069.

References

[1] Rödel J, Webber K G, Dittmer R, Jo W, Kimura M and Damjanovic D 2015 Transferring lead-free piezoelectric ceramics into application *J. Eur. Ceram. Soc.* **35** 1659–81
[2] Mitsui T and Westphal W B 1961 Dielectric and x-ray studies of $Ca_xBa_{1-x}TiO_3$ and $Ca_xSr_{1-x}TiO_3$ *Phys. Rev.* **124** 1354–9

[3] Yu Z, Ang C, Guo R and Bhalla A S 2002 Piezoelectric and strain properties of $Ba(Ti_{1-x}Zr_x)O_3$ ceramics *J. Appl. Phys.* **92** 1489–93

[4] Maiti T, Guo R and Bhalla A S 2008 Structure-property phase diagram of $BaZr_xTi_{1-x}O_3$ system *J. Am. Cer. Soc.* **91** 1769–80

[5] Jeong I K, Park C Y, Ahn J S, Park S and Kim D J 2010 Ferroelectric-relaxor crossover in $Ba(Ti_{1-x}Zr_x)O_3$ studied using neutron total scattering measurements and reverse Monte Carlo modeling *Phys. Rev.* B **81** 214119

[6] Hui W and Jiagang W 2014 Phase transition, microstructure, and electrical properties of Ca, Zr, and Sn-modified $BaTiO_3$ lead-free ceramics *J. Alloys Compd.* **615** 969–74

[7] Kalyani A K, Senyshyn A and Ranjan R 2013 Polymorphic phase boundaries and enhanced piezoelectric response in extended composition range in the lead free ferroelectric $BaTi_{1-x}Zr_xO_3$ *J. Appl. Phys.* **114** 014102

[8] Liu W and Ren X 2009 Large piezoelectric effect in Pb-free ceramics *Phys. Rev. Lett.* **103** 257602

[9] Ye S, Fuh J and Lu L 2012 Effects of Ca substitution on structure, piezoelectric properties, and relaxor behavior of lead-free $Ba(Ti_{0.9}Zr_{0.1})O_3$ piezoelectric ceramics *J. Alloys Compd.* **541** 396–402

[10] Hao J, Bai W, Li W and Zhai J 2012 Correlation between the microstructure and electrical properties in high-performance $(Ba_{0.85}Ca_{0.15})(Zr_{0.1}Ti_{0.9})O_3$ lead-free piezoelectric ceramics *J. Am. Ceram. Soc.* **95** 1998–2006

[11] Sun Z, Pu Y, Dong Z, Hu Y, Wang P, Liu X and Wang Z 2014 Impact of fast microwave sintering on the grain growth, dielectric relaxation and piezoelectric properties on $Ba_{0.18}Ca_{0.02}Ti_{0.09}Zr_{0.10}O_3$ lead-free ceramics prepared by different methods *Mater. Sci. Eng.* B **185** 114–22

[12] Cui Y, Liu X, Jiang M, Zhao X, Shan X, Li W, Yuan C and Zhou C 2012 Lead-free $(Ba_{0.85}Ca_{0.15})(Ti_{0.9}Zr_{0.1})O_3$-$CeO_2$ ceramics with high piezoelectric coefficient obtained by low-temperature sintering *Ceram. Int.* **38** 4761–4

[13] Jiang M, Lin Q, Lin D, Zheng Q, Fan X, Wu X, Sun H, Wan Y and Wu L 2013 Effects of MnO_2 and sintering temperature on microstructure, ferroelectric, and piezoelectric properties of $Ba_{0.85}Ca_{0.15}Ti_{0.90}Zr_{0.10}O_3$ lead-free ceramics *J. Mater. Sci.* **48** 1035–41

[14] Tan C K I, Yao K and Ma J 2013 Effects of LiF on the structure and properties of $Ba_{0.85}Ca_{0.15}Zr_{0.1}Ti_{0.9}O_3$ lead-free piezoelectric ceramics *Int. J. Appl. Ceram. Technol.* **10** 701–6

[15] Reyes-Montero A, Pardo L, López-Juárez R, González A M, Cruz M P and Villafuerte-Castrejón M E 2014 Lead-free $Ba_{0.9}Ca_{0.1}Ti_{0.9}Zr_{0.1}O_3$ piezoelectric ceramics processed below 1300 °C *J. Alloys Compd.* **584** 28–33

[16] Wu J, Xiao D, Wu W, Chen Q, Zhu J, Yang Z and Wang J 2012 Composition and poling condition-induced electrical behavior of $(Ba_{0.85}Ca_{0.15})(Ti_{1-x}Zr_x)O_3$ lead-free piezoelectric ceramics *J. Eur. Ceram. Soc.* **32** 891–8

[17] Tian Y, Chao X, Wei L, Liang P and Yang Z 2013 Phase transition behavior and electrical properties of lead-free $(Ba_{1-x}Ca_x)(Zr_{0.1}Ti_{0.9})O_3$ piezoelectric ceramics *J. Appl. Phys.* **113** 184107

[18] Alemany C, Gonzalez A M, Pardo L, Jimenez B, Carmona F and Mendiola J 1995 Automatic determination of complex constants of piezoelectric lossy materials in the radial mode *J. Phys. D: Appl. Phys.* **28** 945–56

[19] Keeble D S, Benebdallah F, Thomas P A and Maglione M 2013 Revised structural phase diagram of $(Ba_{0.7}Ca_{0.3}TiO_3)$-$(BaZr_{0.2}Ti_{0.8}O_3)$ *Appl. Phys. Lett.* **102** 092903

[20] Jeong I K and Ahn J S 2012 The atomic structure of lead-free $Ba(Zr_{0.2}Ti_{0.8})O_3$-$(Ba_{0.7}Ca_{0.3})TiO_3$ by using neutron total scattering analysis *Appl. Phys. Lett.* **101** 242901

[21] Benabdallah F, Simon A, Khemakhem H, Elissalde C and Maglione M 2011 Linking large piezoelectric coefficients to highly flexible polarization of lead free $BaTiO_3$-$CaTiO_3$-$BaZrO_3$ ceramics *J. Appl. Phys.* **109** 124116

[22] Bharathi B and Varma K B R 2014 Grain and the concomitant ferroelectric domain size dependent physical properties of $Ba_{0.85}Ca_{0.15}Zr_{0.10}Ti_{0.90}O_3$ ceramics using powders derived from oxalate precursor route *J. Appl. Phys.* **116** 164107

[23] Tang X G, Chew K H and Chan H L W 2004 Diffuse phase transition and dielectric tenability of $Ba(Zr_xTi_{1-x})O_3$ relaxor ferroelectric ceramics *Acta Mater.* **52** 5177–83

[24] Uchino K and Nomura S 1982 Critical exponents of the dielectric constants in diffused phase transition crystals *Ferroelectr. Lett. Sect.* **44** 55–61